

# Experimental Results Relating Stress and Birefringence to Strain in Poly(dimethylsiloxane) Networks. Comparisons with Theory

Burak Erman<sup>†</sup> and Paul J. Flory\*

IBM Research Laboratory, San Jose, California 95193. Received February 24, 1983

**ABSTRACT:** Measurements of stress and birefringence as functions of elongation are reported for two poly(dimethylsiloxane) networks differing in degrees of cross-linking. Samples swollen with dodecane, hexadecane, decalin, tetraethylmethane, and carbon tetrachloride were investigated. The dependences of the stress on elongation and on dilation are in full agreement with theoretical calculations based on concise sets of parameters which are determined within narrow ranges solely by the reduced stress  $[f^*]$  in the limit  $\alpha_e^{-1} \rightarrow 0$ ,  $\alpha_e$  being the extension ratio relative to the state of rest. Data for different degrees of swelling converge in this limit to a common intercept  $[f^*_{ph}]$ , the value for the corresponding phantom network, that reflects the degree of cross-linking. Convergence to the same reduced stress at  $\alpha_e = 0$  confirms the theoretical form of the stress-strain relationship. Through arbitrary assignment of the stress-optical coefficient  $C = \lim_{\alpha_e \rightarrow 0} (\Delta n / \tau)$  and reliance on parameters employed for the analysis of stress-strain data, good agreement between the birefringence  $\Delta n$  and the true stress  $\tau$  is achieved. Predicted departures of  $\Delta n$  from proportionality to  $\tau$  are confirmed. The observed dependence of  $C$  on the diluent in swollen samples is attributed to intermolecular correlations that effectively enhance the very small intrinsic optical anisotropy of the dimethylsiloxane unit.

## Introduction

That the birefringence exhibited by polymer networks in the high-elastic state is intimately related to the stress is well-known. Direct proportionality, in accordance with Brewster's law, was predicted<sup>1,2</sup> from the theory of rubber elasticity developed on the premise, now discredited, that transformation of the chain vectors in the network is affine in the macroscopic strain. Numerous experiments appear to support proportionality of the birefringence to the stress in simple elongation.<sup>2</sup> However, the results of Stein and co-workers<sup>3,4</sup> on polybutadiene networks clearly show the relationship to be nonlinear when accurate measurements are carried out over a wide range of elongations. Theory incorporating the effects of constraints on the fluctuations in a real network, and presented in the preceding paper,<sup>5</sup> predicts significant departures from proportionality.

The relationships between stress and strain and between birefringence and strain should be examined in detail as prerequisites to inquiry into the dependence of birefringence on stress. In the work reported in this paper, these relationships were investigated for two poly(dimethylsiloxane) (PDMS) networks of different degrees of cross-linking over the maximum ranges of elongation permitted by integrity of the specimens. Reliable extrapolation to infinite strain, i.e., to  $\alpha_e^{-1} = 0$ , where  $\alpha_e$  is the extension ratio relative to the state of rest, provides the key to the analysis of both the stress-strain and the strain-birefringence data. In this limit, the behavior of the real material should converge to that of the corresponding phantom network, whose theoretical interpretation is straightforward. The theory of the constraints operative in real networks at finite strains predicts sigmoidally curved relationships for both the reduced stress<sup>6,7</sup>  $\tau(V/V_0)^{1/3}/(\alpha_e^2 - \alpha_e^{-1})$  and the reduced birefringence<sup>5</sup>  $\Delta n(V/V_0)^{1/3}/(\alpha_e^2 - \alpha_e^{-1})$  when plotted against  $\alpha_e^{-1}$  for  $\alpha_e > 1$ . The linearity of the reduced stress with  $\alpha_e^{-1}$  prescribed by the much used Mooney-Rivlin relationship is demonstrated to be incorrect by experiments<sup>2</sup> as well as by theory. The sigmoidal inflections of the respective relationships to  $\alpha_e^{-1}$  predicted by recent theory<sup>6,7</sup> extend beyond the range of extension generally accessible to experiment. These relationships, which are of key importance to the analysis of experimental data, can be put to test by conducting experiments on networks swollen to varying degrees.<sup>8</sup> The contributions

of the constraints to both  $\tau$  and  $\Delta n$  in real networks are diminished by dilation (i.e., by swelling); hence the magnitudes of the extrapolations of both the reduced stress and the reduced birefringence are diminished. By comparing values of these quantities measured as functions of strain ( $\alpha_e$ ) on unswollen and swollen specimens of the same material with theoretical calculations carried out with the same values of relevant parameters, the validity of the theoretical relationships of  $\tau$  and of  $\Delta n$  to strain can be ascertained.

Experiments performed in this investigation were motivated by these considerations. Following investigation of the relationships of  $\tau$  and of  $\Delta n$  to the extension ratio  $\alpha_e$ , we turned to the dependence of  $\Delta n$  on  $\tau$ , departures from direct proportionality being compared with predictions of theory.<sup>5</sup>

The limiting value of the stress-optical coefficient  $C \equiv \lim_{\alpha_e \rightarrow 0} (\Delta n / \tau)$  commands special interest because it leads directly to the parameter  $\Gamma_2$  that characterizes the optical anisotropy of the chain under strain; see eq 19 of the preceding paper,<sup>5</sup> hereafter designated I. As formally defined,  $\Gamma_2$  depends on the anisotropies of the polarizabilities  $\bar{\alpha}_i$  of all units  $i$ , or groups, in the chain (see eq I-12). It is well established by experimental measurements on low molecular weight liquids<sup>9-13</sup> and on polymers<sup>14-22</sup> as well that the observed optical anisotropy may include significant contributions from neighboring molecules (e.g., solvent) or chain segments. Such contributions depend on the anisotropy of the polarizability of the neighbor molecule and on its correlation with the solute, or the chain segment, under observation. Consequently, values of  $C$  obtained by extrapolating the birefringences of swollen networks to  $\alpha_e^{-1} = 0$  include effects of correlations that depend on the given solvent and its concentration. Observations are presented on these effects of several diluents in PDMS networks as manifested in values of the stress-optical coefficient  $C$ .

## Experimental Section

**Materials.** Linear PDMS of high molecular weight ( $2 \times 10^6$ ) was obtained from Dow-Corning Co. Cross-linking was carried out by mixing dicumyl peroxide with the polymer on a mill, then molding sheets, ca. 0.8 mm in thickness, in a press, and "curing" at 120 °C for 25 min. Samples A and B were cross-linked with 0.2 and 0.1% (w/w) dicumyl peroxide, respectively.

Diluents were procured from the following sources: carbon tetrachloride, reagent grade, from J. T. Baker Chemical Co.; decalin (cis-trans ratio, 62:38) from Matheson Coleman and Bell; tetraethylmethane, exceeding 99% purity according to vapor phase

<sup>†</sup> Permanent address: School of Engineering, Bogazici University, Bebek, Istanbul, Turkey.

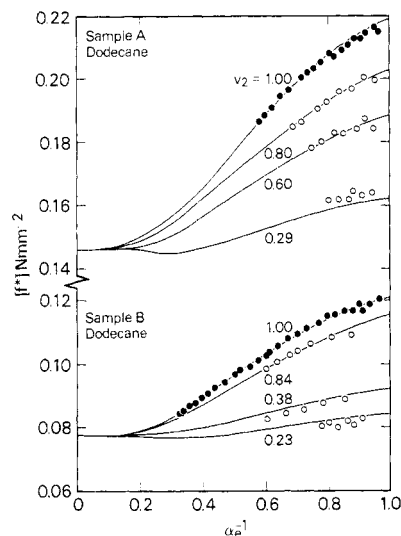


**Figure 1.** Reduced stresses for samples A and B, unswollen (filled circles) and swollen with dodecane (open circles) to the indicated volume fractions  $v_2$  of polymer, plotted against the reciprocal of the extension ratio  $\alpha_e$  relative to the isotropic state of the same volume. The curves have been calculated from theory with a consistent set of parameters for all curves; see text.

chromatography, from Chemical Sample Co.; dodecane and hexadecane from Aldrich Chemical Co.

**Preparation of Specimens.** Strips having dimensions ca.  $30 \times 8 \times 0.8$  mm<sup>3</sup> were cut from the cross-linked sheets. Thicknesses of unswollen specimens were determined by weighing specimens whose lateral dimensions had been measured with a cathetometer: a density of  $0.974$  g cm<sup>-3</sup> for PDMS at  $20^\circ\text{C}$  was used for the conversion.<sup>23</sup>

Partially swollen samples were prepared by immersing strips of the dimensions stated above in the swelling liquid for a limited time and then allowing 24 h for diffusion of the diluent uniformly throughout the specimen. The amount of diluent absorbed was determined by weighing, and the volume fraction  $v_2$  of polymer was calculated from the known density of the liquid and that of PDMS, additivity of volumes being assumed. In the case of samples swollen to equilibrium by immersion, the degree of swelling  $1/v_2$  was determined by comparing the linear dimensions of the swollen and unswollen specimen.

**Mechanical and Optical Measurements.** The tensile force and birefringence were measured concurrently as functions of elongation. Unswollen strips and those partially swollen with varying amounts of dodecane and hexadecane were suspended vertically between two clamps; the upper clamp was fixed, and the lower one suspended a dead weight. Extensions were determined by measuring the distance between fiducial marks, ca. 1.0 cm apart, with a cathetometer (Gaertner 4436-P) having a precision of  $\pm 0.001$  cm. Samples swollen to equilibrium in the more volatile diluents, CCl<sub>4</sub>, tetraethylmethane (TEM), and decalin (Dec), were submerged in the pure liquids in a cylindrical container. The lower clamp was fixed and the upper one was suspended from a strain gauge (Statham, 700-g range). The length, measured as above, was fixed and the force was determined.

Birefringences were determined by using a single-frequency He-Ne laser (Tropel Model 100) according to well-established procedures. The retardation was measured with a Babinet compensator (Karl Lambrecht D/B/A, Crystal Optics, Series No. 170). Details have been presented previously.<sup>20,24</sup>

The strain and birefringence approached steady values within 10–15 min on unswollen samples. In order to ensure attainment of equilibrium, measurements were monitored for 2 h at each load on specimens of sample A; a longer period of 4 h was allowed for sample B, having a lower degree of cross-linking. Although equilibration was more rapid for swollen samples, an interval of at least 2 h was allowed at each load, or each length in the case of immersed samples. All measurements were carried out at  $20^\circ\text{C}$ .

Refractive indices of swollen samples were estimated by considering the specific refractivities to be additive in the volume

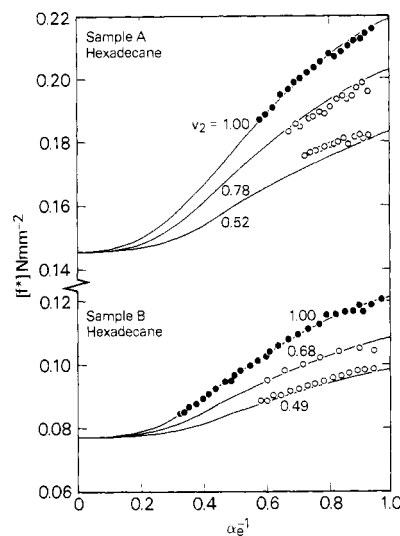


**Figure 2.** Reduced stresses for samples A and B unswollen (filled circles) and swollen with hexadecane (open circles). Curves were calculated from theory. See legend for Figure 1.

fractions of the two components. The refractive index of PDMS was taken to be 1.4066 at  $20^\circ\text{C}$ .<sup>20</sup> Tabulated literature values for the diluents were used.

## Results and Discussion

**Dependence of Stress on Strain and Dilation.** Results of stress-elongation measurements may be analyzed in terms of the reduced nominal stress defined by

$$[f^*] = f^*(V/V_0)^{-1/3}/(\alpha_e - \alpha_e^{-2}) \quad (1)$$

where  $f^*$  is the tensile force per unit area measured in the reference state of volume  $V_0$ ,  $V$  is the volume of the system under conditions of measurement, and  $\alpha_e$  is the extension ratio relative to the length of the sample when at ease at volume  $V$ . Alternatively, one may define a reduced stress according to

$$[\tau] = \tau(V/V_0)^{1/3}/(\alpha_e^2 - \alpha_e^{-1}) \quad (2)$$

where  $\tau$  is the true stress. Thus defined,  $[\tau]$  is equal to  $[f^*]$ . In deference to precedent, we use the symbol  $[f^*]$  for this quantity.

For a phantom network

$$[\tau_{ph}] \equiv [f^*_{ph}] = \xi kT/V_0 \quad (3)$$

where  $\xi$  is the cycle rank of the network, and (see eq I-25)

$$\tau_{ph} = [f^*_{ph}](V/V_0)^{-1/3}(\alpha_e^2 - \alpha_e^{-1}). \quad (4)$$

For networks in general subjected to uniaxial deformation

$$\tau = \tau_{ph} + \tau_c$$

or

$$[\tau] \equiv [f^*] = [f^*_{ph}](1 + \tau_c/\tau_{ph}) \quad (5)$$

where  $\tau_c/\tau_{ph}$  is given by eq I-54.

Results of stress-deformation measurements represented in this manner for the two PDMS samples A and B differing in degrees of cross-linking are plotted against  $\alpha_e^{-1}$  in Figures 1–3. Filled circles denote data for unswollen samples; open circles are for swollen samples. The data for unswollen samples A and B, shown first in Figure 1, are repeated in Figures 2 and 3 in order to afford comparisons with variously swollen samples.

Measurements were performed by successively increasing the load in suitable increments. Specimens were held at each load for the times stated in the Experimental Section in order to ensure satisfactory approach to equilibrium. Swollen samples equilibrated rapidly. That

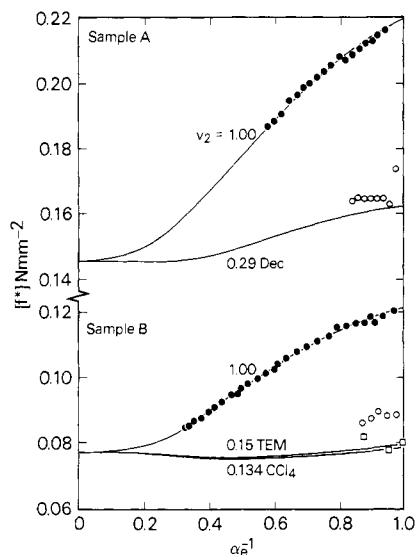


**Figure 3.** Reduced stresses for samples swollen to equilibrium by immersion in decalin (Dec, open circles), tetraethylmethane (TEM, open circles), and  $\text{CCl}_4$  (open squares) as functions of  $\alpha_e^{-1}$ . Data for unswollen samples (filled circles) are repeated from Figures 1 and 2 for comparison. The point at  $\alpha_e^{-1} = 1$  for the sample swollen in  $\text{CCl}_4$  was determined by bending the specimen under small loads. Curves were calculated from theory; see text.

equilibrium was virtually attained for unswollen samples as well as confirmed at several representative data points for both samples A and B by swelling the specimen with cyclohexane vapor to a volume fraction  $1 - v_2$  of diluent exceeding 0.5 and then deswelling in circulating air at 80 °C for 8 h, the length of the specimen being fixed throughout the cycle. The tension measured after swelling and deswelling coincided with the tension previously observed within the precision of measurement.

Results for samples swollen with dodecane (D) and hexadecane (H) are presented in Figures 1 and 2, respectively. Degrees of swelling are denoted by the reciprocals of the volume fractions  $v_2$  of polymer indicated with each curve. The results were obtained by conducting mechanical measurements on the swollen samples suspended in air and, hence, subject to evaporation to the extent determined by volatility of the diluent. Measurements at higher degrees of swelling in dodecane may have been subject to minor vitiation on this account. Experiments using the less volatile diluent, hexadecane, were free from this source of error.

The results in Figure 3 were determined on specimens swollen to equilibrium, the measurements being carried out with the sample immersed in the swelling fluid. Data are shown for sample A swollen in decalin (Dec), for sample B swollen in tetraethylmethane (TEM), and for sample B in  $\text{CCl}_4$ . Equilibrium degrees of swelling determined on unstrained specimens are given by reciprocals of the volume fractions  $v_2$  of polymer network indicated with the respective curves in Figure 3. The data points, obtained for the samples while immersed in the swelling medium, have been corrected for the effect on the stress of the small increase in swelling with extension in the manner described in the Appendix. Thus, the data shown refer to the network swollen to the extent indicated by the quoted value of  $v_2$ . The correction did not exceed 13% in any case.

The experimental point at  $\alpha_e^{-1} = 1$  for sample B swollen with  $\text{CCl}_4$ , shown in the lower portion of Figure 3, was obtained by bending a specimen clamped at one end in a horizontal position while immersed in the diluent. The swollen specimen, with unswollen dimensions of  $20 \times 8 \times 0.80 \text{ mm}^3$ , was deflected vertically, like a cantilever beam,

by a load  $p$  applied at the free end. The Young's modulus  $E$  was calculated from

$$E = (L^3/3I)(p/y) \quad (6)$$

where  $L$  and  $I$  are, respectively, the length and cross-sectional moment of inertia of the sample, and  $y$  is the vertical deflection of the tip of the cantilever beam under load  $p$ . The reduced stress is given for  $\alpha = 1$  by

$$[f^*] = E(V/V_0)^{1/3}/3 \quad (7)$$

The point shown is the average of measurements at five different loadings, each the average of five readings of the displacement. The range of error was less than 5%. The result is confirmatory of other data which are subject to fairly large errors owing to fragility of the fully swollen samples and the difficulties of measuring the small strains realizable without rupture.

The curves shown in Figures 1–3 have been calculated according to eq 3 and 5, above, with  $\tau_c/\tau_{ph}$  furnished by eq I-54 of the preceding paper; the functionality  $\varphi$  of the network was assumed to be four. The required function  $K(\lambda^2)$  was evaluated according to eq I-48. Values of the parameters chosen to optimize agreement with the experimental points for unswollen sample A are  $\xi kT/V_0 = 0.146 \text{ N mm}^{-2}$ ,  $\kappa = 5.5$ , and  $\zeta = 0.05$ . For sample B the parameters so chosen are  $0.077 \text{ N mm}^{-2}$ ,  $7.0$ , and  $0.05$ , respectively. Curves for the swollen samples were calculated by using the same parameters for the respective samples. The volume ratio  $V/V_0$  required by eq I-54 and for the evaluation of  $\lambda_{||}$  and  $\lambda_{\perp}$  according to eq I-23 was identified with the reciprocal of the volume fraction  $v_2$  of polymer in the swollen sample, as indicated with each curve in Figures 1–3. This identification is justified by the fact that the networks were prepared by cross-linking the unswollen polymers; hence the reference volume  $V_0$  is approximated by the volume of the unswollen sample (apart from corrections for thermal contraction, which are negligible for our purposes).

The convex curvature of the reduced stress with  $\alpha_e^{-1}$  predicted by theory is confirmed by the experimental data on the unswollen samples in the range  $0.5 < \alpha_e^{-1} < 1.0$ , and the points extending to lower values of  $\alpha_e^{-1}$  for sample B intimate an inflection denoting a sigmoidal curve. Rupture of the specimens unfortunately precluded extension of the measurements to the higher elongations that would be required to test the course of the relationship predicted<sup>6,7</sup> at smaller  $\alpha_e^{-1}$  and especially to establish the intercept empirically.

The difference between  $[f^*]$  at small strains, i.e., at  $\alpha_e^{-1}$  approaching unity, and the intercept at  $\alpha_e^{-1} = 0$  diminishes with dilation. Hence, measurements on swollen samples set narrower limits on the intercepts. The generally satisfactory agreement between experiments on swollen samples and the curves calculated by using the same parameters as for the unswollen samples is therefore indirectly confirmatory of the sigmoidal shapes of the curves for unswollen samples and of the marked positive curvature predicted<sup>6,7</sup> at  $\alpha_e^{-1} < 0.3$ .

Results on the samples swollen to equilibrium by immersion (Figure 3) should be most decisive on this issue. The difficulties cited above that attend measurements under those conditions led to the larger experimental errors that are evident. The determination in  $\text{CCl}_4$  at  $\alpha_e = 1$ , based on measurements of the deflection of a cantilevered specimen, is believed to be accurate. It yields a value of  $[f^*]$  that approximates the intercept,  $[f^*]_{ph}$ , within narrow limits, as required by theory.

The results presented above, and those examined previously<sup>8</sup> as well, confirm a main premise<sup>25,26</sup> of the current

theory,<sup>6,7</sup> namely, that the effects of the constraints are attenuated by elongation and by dilation and that they should vanish altogether at high extensions and/or dilations. It is noteworthy also that these results give no indication of specific effects of the various diluents, the diverse sizes and shapes of their molecules notwithstanding. Thus, intermolecular correlations manifested in the stress-optical coefficients (cf. seq.) appear to have no discernible effect on the relationship of stress to strain.

The curves in Figures 1–3 representing calculations according to theory are more severely restricted than the presence of three parameters may suggest. On the plausible grounds that the constraints are determined by the degree of interpenetration of chains in the network, the two principal parameters, i.e., the intercept  $[f^*_{ph}] = (\xi kT/V_0)$  and  $\kappa$ , should be related according to<sup>8</sup>

$$\kappa = I(N_A d/2)^{3/2}(\langle r^2 \rangle_0/M)^{3/2}(kT/[f^*_{ph}])^{1/2} \quad (8)$$

where  $N_A$  is Avogadro's number,  $d$  is the density of the polymer,  $\langle r^2 \rangle_0/M$  is the ratio of the mean-squared end-to-end length of the unperturbed chain to its molecular weight, and  $I$  is the interpenetration parameter whose value appears to be<sup>8</sup> ca. 0.50–0.55. The parameters  $[f^*_{ph}]$  and  $\kappa$  chosen above for polymer networks A and B yield  $I = 0.54$  and  $0.50$ , respectively, in good agreement with values found previously for PDMS and other polymers.<sup>8</sup> Thus, the agreement between theory and experiment demonstrated above could have been achieved through the arbitrary choice of only two parameters for each network sample. One of these,  $\zeta$ , is of marginal importance. Its small value  $>0$  implies a somewhat more rapid dissipation of the constraints than affine deformation of the domains would allow.<sup>7</sup> The theoretically calculated curves in Figures 1–3 are predominantly determined, therefore, by a single arbitrary parameter. Moreover, this parameter,  $[f^*_{ph}]$ , may be evaluated independently, in principle, from determination of the network structure leading to the value of the cycle rank  $\xi$  of the network.<sup>8,27</sup> The comparisons between calculations and experimental results afford a much more stringent test of theory than the number of parameters involved would imply.

**Dependence of Birefringence on Strain, Dilation, and Stress.** A reduced birefringence analogous to the reduced stress may be defined by

$$[\Delta n] = \Delta n(V/V_0)^{1/3}(\alpha_e^2 - \alpha_e^{-1})^{-1} \quad (9)$$

for uniaxial deformation. For a phantom network (see eq I-24)

$$[\Delta n_{ph}] = (\xi kT/V_0)C \quad (10)$$

where  $C$  is formally defined by eq I-19. For a real network under uniaxial deformation (see eq I-45)

$$[\Delta n] = [\Delta n_{ph}](1 + \Delta n_c/\Delta n_{ph}) \quad (11)$$

where  $\Delta n_c/\Delta n_{ph}$  is given by eq I-53.

Primary results of the birefringence measurements, carried out concurrently with the stress measurements, are presented in Figures 4 and 5 for samples A and B, respectively, the reduced birefringence being plotted against  $\alpha_e^{-1}$ . Filled circles represent experimental results for unswollen specimens;<sup>28</sup> other points represent networks swollen with the diluents indicated by the designations used in Figures 1–3.

The curves in Figures 4 and 5 for unswollen samples (with data points shown by filled circles) were calculated according to eq 11 and I-53. The same values of  $\kappa$  and  $\xi$  used for the stress-strain calculations and quoted in the preceding section were employed in these calculations.

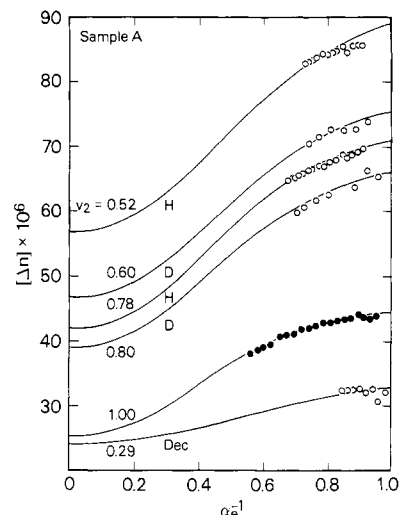


**Figure 4.** Reduced birefringences shown as functions of the reciprocal of the extension ratio  $\alpha_e$  for sample A unswollen (filled circles) and swollen (open circles) in hexadecane (H), dodecane (D), and decalin (Dec) to the extents indicated by the volume fractions  $v_2$  of polymer. Curves were calculated according to theory; see text.

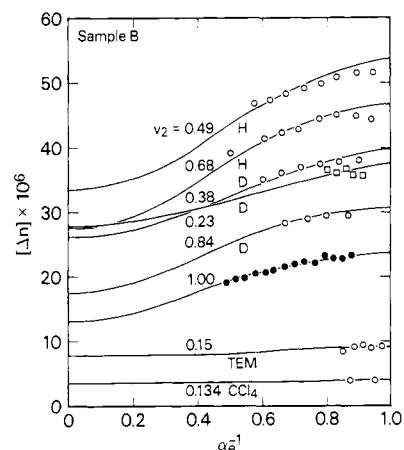


**Figure 5.** Reduced birefringences for sample B unswollen and swollen in the four liquids indicated. See legend to Figure 4.

The additional parameter  $b$  governing the contribution from compliances in the domains of constraint<sup>5</sup> was assigned the value 0.5. As Figures 1 and 2 of the preceding paper<sup>5</sup> show, the calculations are relatively insensitive to this parameter, except at high dilutions. The intercepts  $[\Delta n_{ph}]$  were set equal to  $2.51 \times 10^{-5}$  and  $1.32 \times 10^{-5}$  for networks A and B, respectively. These values were deliberately chosen to be in the same ratio as the intercepts  $[f^*_{ph}] = \xi kT/V_0$  used in the analysis of stress-strain data for the respective samples. It follows from eq 10 that the same value of the stress-optical parameter,  $C = 1.72 \times 10^{-4} \text{ mm}^2 \text{ N}^{-1}$ , applies to both samples, as theory requires.

The curves calculated for the unswollen samples reproduce the data shown in Figures 4 and 5 satisfactorily. The slopes and intimations of curvature in the experimental data are well represented. The ranges covered by the data are insufficient for direct determination of  $[\Delta n_{ph}]$  by empirical extrapolation to  $\alpha_{ph}^{-1} = 0$ . Because of specific effects of diluents on  $C$  (cf. seq.), dilution does not provide a means for determining the intercept, in analogy to the method applied to the stress. It is noteworthy, nevertheless, that only two parameters,  $C$  and  $b$ , beyond those evaluated in the analysis of the stress-strain results serve to determine both curves, and the role of one of these parameters,  $b$ , is minor. The agreement achieved suffices

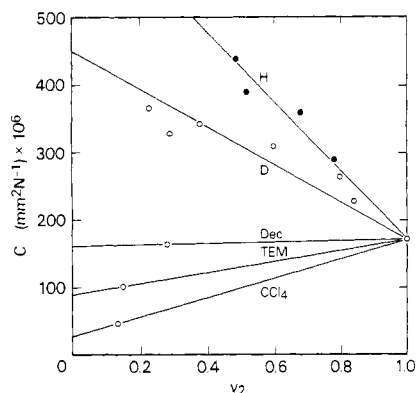


**Figure 6.** Stress-optical coefficients  $C$ , representing values of  $[\Delta n]/[f^*] = \Delta n/\tau$  in the limit  $\alpha_e^{-1} = 0$ , plotted against composition expressed by the volume fraction  $v_2$  of polymer. Values of  $C$  are from the intercepts in Figures 3–5. The lines are drawn on the assumption of linear relationships.

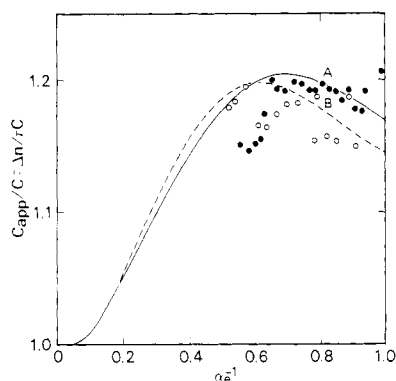


**Figure 7.** Stress-birefringence ratios  $\Delta n/\tau = C_{app}$  divided by  $C$ , the limiting value of that ratio, plotted against  $\alpha_e^{-1}$  for unswollen samples A (filled circles) and B (open circles). Curves have been calculated according to theory; see text.

to demonstrate that  $C$  is not appreciably dependent on strain and degree of cross-linking. Corresponding constancy of the molecular optical anisotropy parameter  $\Gamma_2$  defined by eq I-12 is implied according to eq I-19.

The data for swollen samples require intercepts  $[\Delta n_{ph}] = (\xi kT/V_0)C$  that vary widely, depending both on the diluent and on its concentration. Values of the intercepts were chosen separately for each set of data, therefore. Other parameters were assigned the same values as above. The individual sets of results on the variously swollen samples are insufficient for definitive comparisons with the theoretical curves. Values of  $C$  calculated from the intercepts and the values of  $[f^*] = \xi kT/V_0$  given above form a consistent pattern, however. This is shown in Figure 6, where the values of  $C$  are plotted against the volume fractions  $v_2$  for the several diluents. The results in decalin (Dec) and  $\text{CCl}_4$  are in agreement with those of Liberman et al.<sup>20</sup> when expressed equivalently. We postpone further discussion of these results to the final section of the paper.

In Figure 7 the ratio of the apparent stress-optical coefficient

$$C_{app} \equiv \Delta n/\tau$$

to the intercept  $C$  is plotted against  $\alpha_e^{-1}$ . The data points are for unswollen networks A (filled circles) and B (open circles). The solid and dashed curves have been calculated by using parameters applicable to samples A and B, respectively (see above), with  $b = 0.5$  for both curves. The departure of the ratio plotted on the ordinate from unity represents the contribution of the constraints to the bi-

**Table I**  
Stress-Optical Parameters for PDMS-Diluent Mixtures

diluent	$C \times 10^4$ at $v_2 = 0$ , $\text{mm}^2 \text{N}^{-1}$	$\Gamma_2^0 + a_1$ , $\text{\AA}^3$	$a_1$ , $\text{\AA}^3$
$\text{CCl}_4$	0.27	0.04	(0)
TEM	0.89	0.14	0.10
decalin	1.61	0.24	0.20
dodecane	4.5	0.70	0.66
hexadecane	6.8	1.05	1.01

refrindex relative to the birefringence for the phantom network; compare Figure 3 of I. Owing to the small optical anisotropy of PDMS and the correspondingly small birefringence, the scatter is large. Detailed comparisons with theory therefore are not possible. Positive curvature in the birefringence–stress relationship for networks formed by end-linking polybutadiene chains trifunctionally has been demonstrated recently by Stein, Farris, Kumar, and Soni.<sup>4</sup> The departure from direct proportionality they observe is qualitatively similar to our observations on tetrafunctional PDMS networks, but larger in magnitude.

#### Intermolecular Effects on the Optical Anisotropy.

The optical anisotropy tensors  $\hat{\alpha}_i$  entering into  $C$  via  $\Gamma_2$ , defined by eq I-12, although attributed formally to the chain units, generally include contributions, sometimes large, from neighboring molecules correlated with them, as we have pointed out in the Introduction. Such contributions are manifested in the depolarized Rayleigh scattering,<sup>13,22,29</sup> in the strain birefringence,<sup>14–21</sup> and in other properties that depend on the optical anisotropy.<sup>30,31</sup> Correlative effects may involve units of neighboring chains as well as molecules of the diluent. They are believed to depend on the optical anisotropy of the neighboring molecule expressed by the tensor  $\hat{\alpha}$  and on asymmetry in the shape of this molecule.

On the grounds that correlations with a given unit should be linear, in first approximation, in the concentration of interacting species, we may write

$$\Gamma_2 = \Gamma_2^0 + a_1(1 - v_2) + a_2v_2 \quad (12)$$

where  $\Gamma_2^0$  is considered to represent the intrinsic contributions of the units of the chain exclusive of intermolecular and interchain correlations. (Intramolecular correlations with units in the same chain are taken into account in the evaluation of the summation in eq I-12 and in averaging over all chain configurations.) The second and third terms in eq 12 represent contributions from correlations with diluent and with units of neighboring chains, respectively;  $a_1$  and  $a_2$  express the intensities of these contributions. A corresponding relation could be written for  $C$  expressed as a function of composition.

Results of the birefringence measurements on swollen networks are plotted in Figure 6 in the manner of eq 12. The intercepts at  $v_2 = 0$  yield  $\Gamma_2^0 + a_1$ , with the aid of eq I-19. The common intercept at  $v_2 = 1$  gives  $\Gamma_2^0 + a_2$ . The parameter  $a_1$  should be expected to vanish for an optically isotropic diluent such as  $\text{CCl}_4$ ; hence the intercept at  $v_2 = 0$  should give  $\Gamma_2^0$ . However, TEM is also isotropic in each of the two conformations of low energy accessible to this molecule,<sup>32</sup> yet its intercept is much larger than that for  $\text{CCl}_4$ .

Quantities evaluated from the plots in Figure 7 are assembled in Table I. The intercepts at  $v_2 = 0$  are given in the second column and the quantities  $\Gamma_2^0 + a_1$  deduced from them according to eq I-19 and eq 12 are given in the third column. On the assumption that PDMS at high dilution in  $\text{CCl}_4$  is unaffected by intermolecular correlations (i.e., that  $a_1 = 0$  in this diluent), the parameter  $\Gamma_2^0$

Table II  
Interaction Parameters Calculated  
from Swelling Equilibrium

polymer/diluent	$v_2$ , at equil	$\chi$
A/decalin (Dec)	0.29	0.5401
B/TEM	0.150	0.4388
B/CCl <sub>4</sub>	0.134	0.4538

expressing the intrinsic optical anisotropy of PDMS is 0.04 Å<sup>3</sup>. Subtraction of this very small quantity from others in the third column gives the values of the correlation parameter for the other diluents listed in the last column of the table. If  $\Gamma_2^0 + a_1$  for TEM, or the mean for TEM and CCl<sub>4</sub>, should be identified with  $\Gamma_2^0$ , values in the last column would be decreased accordingly. Regardless of the validity of the identification of the intrinsic optical anisotropy parameter  $\Gamma_2^0$  with the result for CCl<sub>4</sub>, the correlative effects are seen to increase with asymmetry of the diluent.

For undiluted PDMS,  $\Gamma_2 = 0.27$  Å<sup>3</sup>. According to eq 12, this quantity should be identified with  $\Gamma_2^0 + a_2$ . From the value of  $\Gamma_2^0$  above, we thus obtain  $a_2 = 0.23$  for the contribution of intermolecular effects in undiluted PDMS.

On the premise of constitutive additivity of polarizabilities of structural units in the PDMS chain, the anisotropy of the polarizability tensor for any conformation should be proportional to the quantity<sup>20,33</sup>  $\Delta\alpha_{\text{DMS}}$  defined by

$$\Delta\alpha_{\text{DMS}} = \Delta\alpha_{\text{Si-O}} - \Delta\alpha_{\text{Si-C}} + \Delta\alpha_{\text{C-H}} \quad (13)$$

where the  $\Delta\alpha$ 's on the right-hand side are differences between polarizabilities parallel and perpendicular to the bonds denoted by subscript. Upon averaging over all conformations on the basis of rotational isomeric state analysis of PDMS, Liberman et al.<sup>20</sup> found

$$\Gamma_2 = 2.28\Delta\alpha_{\text{DMS}} \quad (14)$$

It follows from the foregoing results, interpreted in the manner above, that  $\Delta\alpha_{\text{DMS}} \approx 0.018$  Å<sup>3</sup>, an exceptionally low value when compared with 0.53 Å<sup>3</sup> for the contribution of the CH<sub>2</sub> unit of a polymethylene chain.<sup>13</sup> Most of the anisotropy of the PDMS chain, as manifested in its strain birefringence, appears to be attributable to intermolecular effects.

These inferences are being pursued through further measurements on PDMS that include depolarized Rayleigh scattering and electric birefringence.

**Acknowledgment.** We take pleasure in acknowledging the indispensable assistance of Dr. Harold Leeper of ALZA Corp., Palo Alto, CA, who prepared the cross-linked samples A and B used in this investigation.

## Appendix A. Swelling Equilibrium in Networks and the Effect of Longitudinal Strain Thereon

The chemical potential of the diluent in a swollen network, treated as a semiopen thermodynamic system, consists of the sum of two contributions: one due to mixing (dilution) and the other to the elastic response of the network.<sup>34</sup> The former, expressed as the difference from the chemical potential  $\mu_1^0$  of the pure diluent, is given by

$$(\mu_1 - \mu_1^0)_{\text{mix}} = RT[\ln(1 - v_2) + v_2 + \chi v_2^2] \quad (\text{A-1})$$

where  $R$  is the gas constant,  $v_2$  is the volume fraction of polymer in the swollen network, and  $\chi$  is the familiar interaction parameter. For isotropic dilation, the second contribution can be evaluated according to

$$(\mu_1 - \mu_1^0)_{\text{el}} = (\partial\Delta A_{\text{el}}/\partial\lambda^2)_{T,p}(\partial\lambda^2/\partial n_1)_{T,p} \quad (\text{A-2})$$

where  $\Delta A_{\text{el}}$  is the elastic free energy,  $n_1$  is the number of solvent molecules, and  $\lambda = \lambda_x = \lambda_y = \lambda_z$  is the isotropic extension ratio given by

$$\lambda = [(n_1\bar{V}_1 + V_0)/V_0]^{1/3} = v_2^{-1/3} \quad (\text{A-3})$$

(see eq I-23), where  $\bar{V}_1$  is the molar volume of the diluent and  $V_0$ , the reference volume, is identified with the volume of the unswollen polymeric network. Evaluating the first of the partial derivatives in eq A-2 from the elastic free energy as given in ref 6 and 7 and the second one from eq A-3, we obtain

$$(\mu_1 - \mu_1^0)_{\text{el}} = (\xi kT/V_0)(\bar{V}_1/\lambda)[1 + (\varphi/2 - 1)^{-1}K(\lambda^2)] \quad (\text{A-4})$$

where  $(\varphi/2 - 1)^{-1}$  replaces the ratio of the number  $\mu$  of junctions to  $\xi$  and  $K(\lambda^2)$  is defined by eq I-48. The first term (unity) in the brackets in eq A-4 represents the part of this expression attributable to the phantom network; the second term is that due to the constraints.

The chemical potential of the diluent in the swollen network is given by the sum of eq A-1 and A-4. Equilibrium requires  $\mu_1 = \mu_1^0$  and hence that this sum must equate to zero, i.e., that

$$RT[\ln(1 - v_2) + v_2 + \chi v_2^2] + (\xi kT/V_0)(\bar{V}_1/\lambda)[1 + (\varphi/2 - 1)^{-1}K(\lambda^2)] = 0 \quad (\text{A-5})$$

For a tetrafunctional network  $\varphi/2 - 1 = 1$ , and eq A-5 reduces to the equation given previously.<sup>8</sup>

If the sample is first swollen to total volume  $V$  and then elongated by the extension ratio  $\alpha_e$  with  $V$  fixed (closed system), then according to eq I-23

$$\lambda_{\parallel} = (V/V_0)^{1/3}\alpha_e = \alpha_e v_2^{-1/3} \quad (\text{A-6})$$

Suppose that swelling was carried to equilibrium with the pure diluent before extension; then  $v_2$  in eq A-6 is the solution of eq A-5; i.e.,  $v_2$  and the associated total volume  $V$  represent the values for isotropic swelling to equilibrium with the pure diluent. Consider extension by  $\alpha_e$  to occur at volume  $V$ . Then let equilibrium be reestablished through exchange between the swollen sample and the pure diluent. Inasmuch as the length is fixed, further swelling (or deswelling if  $\alpha_e < 1$ ) must occur laterally. The transverse extension ratio relative to the state of reference becomes

$$\lambda_{\perp} = (V/V_0)^{1/3}(V'/V)^{1/2}\alpha_e^{-1/2} = \alpha_e^{-1/2}v_2^{1/6}(v_2')^{-1/2} \quad (\text{A-7})$$

where  $V'$  and  $v_2'$  are the total volume and volume fraction, respectively, reached at equilibrium under the conditions stated. The extension ratio relative to the isotropic state of volume  $V'$  is

$$\alpha_e' = \alpha_e(v_2'/v_2)^{1/2} \quad (\text{A-8})$$

and  $\lambda_{\parallel}$  and  $\lambda_{\perp}$  are related to  $\alpha_e'$  and  $v_2' = (V_0/V')$  according to eq I-23.

The elastic contribution to the chemical potential for the sample at fixed length, i.e., at fixed  $\lambda_{\parallel}$ , is

$$(\mu_1 - \mu_1^0)_{\text{el},\lambda_{\parallel}} = (\partial\Delta A_{\text{el}}/\partial\lambda_{\perp}^2)_{T,p,\lambda_{\parallel}}(\partial\lambda_{\perp}^2/\partial n_1)_{T,p,\lambda_{\parallel}} = (\xi kT/V_0)\bar{V}_1\lambda_{\perp}^2 v_2'^2[1 + (\varphi/2 - 1)^{-1}K(\lambda_{\perp}^2)] \quad (\text{A-9})$$

Combination with eq A-1 with  $v_2$  replaced by  $v_2'$  gives  $RT[\ln(1 - v_2') + v_2' + \chi(v_2')^2] +$

$$(\xi kT/V_0)\bar{V}_1\lambda_{\perp}^2 v_2'^2[1 + (\varphi/2 - 1)^{-1}K(\lambda_{\perp}^2)] = 0 \quad (\text{A-10})$$

at equilibrium with pure diluent subject to the condition that  $\lambda_{\parallel}$  is fixed.

From the volume fractions  $v_2$  given in Figure 3 for isotropic swelling to equilibrium in the several diluents, to-

gether with the values of the parameters  $\xi kT/V_0$ ,  $\kappa$  and  $\zeta$  that characterize networks A and B, respectively (see text), one may evaluate  $\chi$  by solution of eq A-5. Results are given in Table II.

Equation A-10 in conjunction with A-7 may be solved iteratively for  $\nu_2'$ , given the network parameters, the value of  $\chi$ , and the extension ratio  $\alpha_e$  relative to the system swollen to equilibrium under isotropic conditions. The reduced force that would obtain if further swelling did not occur as a result of the elongation  $\alpha_e$  may be calculated according to eq 5 and eq I-54 of the preceding paper, with  $V/V_0$  therein equated to  $1/\nu_2$  and with  $\lambda_{\parallel}$  and  $\lambda_{\perp}$  determined by  $\alpha_e$  and  $V/V_0$  according to eq I-23. Repetition of the calculation with  $V'/V_0 = 1/\nu_2'$ ,  $\alpha_e'$  given by eq A-8,  $\lambda_{\perp}$  given by eq A-7, and  $\lambda_{\parallel}$  the same as above, yields the calculated reduced stress for the semiopen system at fixed length. The difference between the latter calculation and the former one gives the correction that should be subtracted from the observed reduced stress. Results shown in Figure 3 were corrected in this manner.

## References and Notes

- (1) Kuhn, W.; Gr $\ddot{u}$ n, F. *Kolloid. Z.* **1942**, *101*, 248.
- (2) Treloar, L. R. G. "The Physics of Rubber Elasticity", 3rd ed.; Clarendon Press: Oxford, 1975.
- (3) Ong, C. S.; Stein, R. S. *J. Polym. Sci., Polym. Phys. Ed.* **1974**, *12*, 1599.
- (4) Stein, R. S.; Farris, R. J.; Kumar, S.; Soni, V. *ACS Symp. Ser.* **1982**, No. 193, 453.
- (5) Erman, B.; Flory, P. J. *Macromolecules*, preceding paper in this issue.
- (6) Flory, P. J. *J. Chem. Phys.* **1977**, *66*, 5720.
- (7) Flory, P. J.; Erman, B. *Macromolecules* **1982**, *15*, 800.
- (8) Erman, B.; Flory, P. J. *Macromolecules* **1982**, *15*, 806.
- (9) Benoit, H.; Stockmayer, W. H. *J. Phys. Radium* **1956**, *17*, 21.
- (10) Prins, J. A.; Prins, W. *Physica (Amsterdam)* **1957**, *23*, 253.
- (11) Kielich, S. *Acta Phys. Polonica* **1960**, *19*, 149; *J. Chem. Phys.* **1967**, *46*, 4090.
- (12) Coumou, D. J.; Hijmans, J.; Mackor, E. L. *Trans. Faraday Soc.* **1964**, *60*, 2244. Coumou, D. J. *Ibid.* **1969**, *65*, 2654.
- (13) Patterson, G. D.; Flory, P. J. *J. Chem. Soc., Faraday Trans. 2* **1972**, *68*, 1098.
- (14) Gent, A. N.; Vickroy, V. V. *J. Polym. Sci., Polym. Phys. Ed.* **1967**, *5*, 47.
- (15) Gent, A. N. *Macromolecules* **1969**, *2*, 262.
- (16) Ishikawa, T.; Nagai, K. *J. Polym. Sci., Polym. Phys. Ed.* **1969**, *7*, 1123. *Polymer J.* **1970**, *1*, 116.
- (17) Gent, A. N.; Kuan, T. H. *J. Polym. Sci., Polym. Phys. Ed.* **1971**, *9*, 927.
- (18) Fukuda, M.; Wilkes, G. L.; Stein, R. S. *J. Polym. Sci., Polym. Phys. Ed.* **1971**, *9*, 1417.
- (19) Rehage, G.; Schäfer, E. E.; Schwarz, J. *Angew. Makromol. Chem.* **1971**, *16/17*, 231.
- (20) Liberman, M. H.; Abe, Y.; Flory, P. J. *Macromolecules* **1972**, *5*, 550.
- (21) Liberman, M. H.; DeBolt, L. C.; Flory, P. J. *J. Polym. Sci., Polym. Phys. Ed.* **1974**, *12*, 187.
- (22) Flory, P. J. *Faraday Discuss. Chem. Soc.* **1979**, *68*, 14.
- (23) Shih, H.; Flory, P. J. *Macromolecules* **1972**, *5*, 758.
- (24) Erman, B.; Marvin, D. C.; Irvine, P. A.; Flory, P. J. *Macromolecules* **1982**, *15*, 664.
- (25) Ronca, G.; Allegra, G. *J. Chem. Phys.* **1975**, *63*, 4990.
- (26) Flory, P. J. *Proc. R. Soc. London, Ser. A* **1976**, *351*, 351.
- (27) Flory, P. J. *Polymer* **1979**, *20*, 1317.
- (28) Birefringence measurements on unswollen sample B at higher extensions, i.e., for  $\alpha_e^{-1} < 0.48$ , were subject to errors due to extraneous effects of scattering of the beam from the boundaries of the sample. This was a consequence of the small width of the specimen under these conditions.
- (29) Fischer, E. W.; Strobl, G. R.; Dettenmaier, M.; Stamm, M.; Steidl, N. *Faraday Discuss. Chem. Soc.* **1979**, *68*, 26.
- (30) Le Fèvre, R. J. W. *Rev. Pure Appl. Chem.* **1970**, *20*, 67.
- (31) Ingwall, R. T.; Czurylo, E. A.; Flory, P. J. *Biopolymers* **1973**, *12*, 1137.
- (32) One of the two conformations of tetraethylmethane (TEM) may be viewed as the fusion of two *n*-pentane chains at their central atoms when both chains are trans,trans. This conformation is asymmetric in shape, being oblate ellipsoidal in form, but its polarizability tensor should be isotropic. The other eligible conformation formed from this one by gauche rotations of opposite signs about two of the central bonds possesses tetrahedral symmetry and therefore is roughly spherical. Its polarizability also should be isotropic.
- (33) In the approximation of tetrahedral symmetry about Si and C, the tensor for the anisotropic part of the polarizability of the structural unit O-Si(CH<sub>3</sub>)<sub>2</sub>-O is
 
$$\hat{\alpha} = \Delta\alpha \text{diag} \left( \frac{2}{3}, 0, -\frac{2}{3} \right)$$
 where  $\Delta\alpha$  is defined by eq 13 and the principal axes in the order of the diagonal elements are taken parallel to O...O, perpendicular thereto in the plane defined by the Si-O bonds, and parallel to CH<sub>3</sub>...CH<sub>3</sub>, respectively. The anisotropy tensor for the PDMS chain as a whole in any conformation is a linear combination of the group tensors so defined, additivity of these tensors for individual units being assumed.
- (34) Flory, P. J.; Rehner, J., Jr. *J. Chem. Phys.* **1943**, *11*, 521. Flory, P. J. *Trans. Faraday Soc.* **1961**, *57*, 829. Flory, P. J.; Tatara, Y. *J. Polym. Sci., Polym. Phys. Ed.* **1975**, *13*, 683.

## More on the Model Parameters of Helical Wormlike Chains

Motoharu Fujii, Kyosuke Nagasaka, Jiro Shimada, and Hiromi Yamakawa\*

Department of Polymer Chemistry, Kyoto University, Kyoto, Japan.

Received January 11, 1983

**ABSTRACT:** The model parameters of the helical wormlike chains corresponding to various real polymer chains, both flexible and stiff, are determined from a comparison with the rotational isomeric state models or from an analysis of experimental data for equilibrium and transport properties. Then some general aspects of the behavior of the model parameters are discussed. This serves to guess their probable ranges for a given new polymer. The results are useful in a study of the chain dynamics recently initiated on the basis of the discrete helical wormlike chain.

## I. Introduction

In recent years, we have shown that the helical wormlike (HW) chain<sup>1-3</sup> can mimic the equilibrium conformational behavior of real chains as well as the rotational isomeric state (RIS) model.<sup>4</sup> However, the RIS model or conventional bond chains are not necessarily convenient for the treatment of steady-state transport and dynamic properties of real chains, both flexible and stiff. Thus, we have

evaluated the steady-state transport coefficients on the basis of the HW cylinder model.<sup>5,6</sup> Further, we have recently started a study of the dynamics of dilute polymer solutions on the basis of the discrete HW chain<sup>7-9</sup> whose equilibrium conformational behavior is almost identical with that of the (continuous) HW chain. In order to proceed to make an extensive analysis of, for instance, local motions of various real chains, as probed from dielectric